# The scattering of He atoms from a microstructured grating: Quantum reflection probabilities and diffraction patterns

**Salvador Miret-Artés**[*,†] and **Eli Pollak**[*,‡]

*Instituto de Física Fundamental, Consejo Superior de Investigaciones Científicas, Serrano 123, 28006 Madrid, Spain*

*, and Chemical Physics Department, Weizmann Institute of Science, 76100, Rehovot, Israel*

E-mail: s.miret@iff.csic.es; eli.pollak@weizmann.ac.il

[*]To whom correspondence should be addressed

[†]Instituto de Física Fundamental, Consejo Superior de Investigaciones Científicas, Serrano 123, 28006 Madrid, Spain

[‡]Chemical Physics Department, Weizmann Institute of Science, 76100, Rehovot, Israel

**Abstract**

The quantum reflection measured previously by Zhao et al (Phys. Rev. A, **2008**, *78*, 010902(R)) for the scattering of He atoms off a microstructured grating is described and analyzed theoretically. Using the close-coupling formalism with a complex absorbing potential and describing the long range interaction in terms of the Casimir-van der Waals potential, we find probabilities and diffraction patterns which are in fairly good agreement with the experimental results. The central outcomes of this study are two fold. First is the theoretical confirmation that indeed, the phenomenon of quantum reflection may be detected not only through the elastic peak but also in terms of a quantum reflected diffraction pattern. Secondly, we demonstrate that the phenomenon of quantum reflection is the result of a coherent process where all the potential regions are involved on an equal footing. It is a nonlocal property and cannot be related only to the long range badlands region of the potential of interaction.

As described by Friedrich and Jurisch[1] "quantum reflection ... refers to the classically forbidden reflection of a particle in a classically allowed region without classical turning points and can occur in the attractive tails of atom-atom or atom-surface potentials." A similar description claims that "Quantum reflection is a process in which a particle reflects from a potential without reaching a classical turning point".[2] This quantum reflection probability increases with low kinetic energies or incident velocities, approaching unity at threshold. It has been observed experimentally for He atoms, dimers and trimers scattered from a microstructured grating at very low kinetic energies and grazing angles.[3,4] It has also been measured experimentally through the diffraction pattern of He atoms scattered from a microstructured grating.[3] It was specifically claimed in Ref.[4] that the quantum reflection of He dimers occurs several nanometers above the surface grating. The effect is sometimes termed as a quantum suppression effect because presumably the contact between the two partners of the collision is suppressed.

Total reflection probabilities and diffraction intensities are usually described theoretically in terms of the long-range Casimir-van der Waals potential tail and, in general, for potentials falling off faster than $r^{-2}$.[6] At this near-threshold condition, semiclassical theories break down.[7] In particular, the WKB approximation is not expected to work well far away from the surface since the local de Broglie wavelength is not slowly varying. By considering the modified Schrödinger equation for which the WKB wave function is an exact solution, it is possible to infer the region where the WKB approximation is poor. This *local property* is given by a function $Q(r)$ also called the quantality or badlands function which is always real (positive and negative) involving the first two derivatives of the local classical momentum. In regions of high quantality, quantum effects are important and, therefore, quantum reflection is expected to be dominant in the corresponding scattering. For He atom scattering, the badlands region of the potential is typically located at distances of several hundreds (or even thousands) of atomic units from the surface. By considering the time delay,[7] which is much shorter than the classical time delay, one infers that effectively the reflection occurs

far away from the surface. Recently, it has been theoretically shown that the scattering of light particles (with a static polarizability) from periodically distributed charge dopants on flat surfaces can also exhibit quantum reflection.[8]

In this work, we will demonstrate that quantum reflection may show up in the diffraction pattern. Not less important is our observation that the reflection is not a local property and is not determined only by the long range interaction potential and the badlands region of the attractive potential. We find that the interaction between the He atoms and the grating or, in general, the surface is critical for obtaining reflection probabilities and diffraction patterns displaying fairly good agreement with the experimental results. The coherent process involving such a reflection can not be theoretically described by the van der Waals and Casimir potential tail alone, the inner part of the interaction potential plays an important role. By using the close-coupling (CC) formalism,[9] which is a numerically exact method, we find that the quantum reflection is a coherent process involving the full potential region and, therefore, it can only be considered as a *nonlocal property*. As the CC formalism is by definition unitary, absorbing boundary conditions are used to suppress the reflection component coming from the inner repulsive part of the potential. This is carried out by using the so-called complex absorbing potentials.[10,11] The basic strategy is to introduce an imaginary potential which is essentially zero in the physically relevant interaction region and is turned on at the edge of the coordinate grid for numerical integration.

In the experiment, the reflection grating, which is assumed to be in the $x$-direction, consists of a 56-mm-long microstructured array of 110-nm-thick, 10 $\mu$m-wide and 5-mm-long parallel chromium strips on a flat quartz substrate.[3,4] The center-to-center distance of the strips, and thereby the period, $d$, is 20 $\mu$m. Given this geometry, the quartz surface between the strips is completely shadowed by the strips for all the incidence angles used. A chromium oxide surface is expected to be formed while the grating is exposed to air before mounting it in the apparatus. Diffraction patterns were measured at different source temperatures $T_0$ (ranging from 14 K up to 31 K) and pressures around $P_0 = 6$ bar were also reported. In the

cryogenic free jet expansion of He atoms, the incident energy is given by $E_i = (5/2)k_B T_0$ where $k_B$ is the Boltzmann constant .[5] The incident grazing angle $\theta_i$ is varied between 3 and 15 $mrad$ and measured with respect to the grating surface plane. The diffraction angles $\theta_n$ are given by the conservation of the momentum or Bragg's law in terms of wave vectors

$$cos\theta_i - cos\theta_n = \frac{n\lambda}{d} \tag{1}$$

where $\lambda$ is the de Broglie wave length of the incident particle and the diffraction order is given by $n$. Negative diffraction orders correspond to diffraction angles close to the surface grating. Final results are usually plotted as a function of the corresponding perpendicular wave vector along the $z$-direction

$$k_{perp} \simeq \frac{\sqrt{5mk_B T_0}}{\hbar}\, sin\theta_i \tag{2}$$

where $m$ is the mass of the incident particle. A detailed theoretical model correctly accounting for the atom-surface interaction potential would be needed to determine the corresponding parameters from the experimental data.

In this work, the interaction potential is modelled by a product of two functions

$$U(x,z) = V(z)h(x) \tag{3}$$

where the first factor $V(z)$ takes into account the interaction along the perpendicular coordinate $z$ and the second factor $h(x)$ describes the periodic grating by means of an infinite series of squared pulses along the horizontal coordinate $x$. The first factor is assumed to be a Morse potential, $V_M(z)$, at short distances, and an attractive Casimir-van der Waals

potential $V_C$, at large distances, written as

$$V(z) \;=\; \begin{cases} V_M(z) = D\left[e^{-2\chi z} - 2e^{-\chi z}\right] & , z < \bar{z} \\ V_C(z) = -\frac{C_4}{(l+z)z^3} & , z \geq \bar{z} \end{cases} \tag{4}$$

where $C_4 = C_3 l$, $C_3$ is the vdW coefficient and $l$ a characteristic length ($l = 9.3$ nm for $He^3$) indicating the transition from the vdW ($z \ll l$) to the Casimir ($z \gg l$) regime. The matching point $\bar{z}$ and the well depth of the Morse potential are determined by imposing the continuity condition for the interaction potential ($V_M(z) = V_C(z)$) and its first derivative ($V'_M(z) = V'_C(z)$):

$$V'(z) \;=\; \begin{cases} V'_M(z) = D\left[-2\chi e^{-2\chi z} + 2\chi e^{-\chi z}\right] & , z < \bar{z} \\ V'_C(z) = \frac{C_4(4z+3l)}{(l+z)^2 z^4} & , z \geq \bar{z} \end{cases} \tag{5}$$

By denoting $x = \chi\bar{z}$ and $L = \chi l$, the resulting dimensionless continuity equation is given by

$$e^x = \frac{1}{2} - \frac{1}{2\left[\frac{3}{x} + \frac{1}{L+x} - 1\right]}. \tag{6}$$

The $C_3$ parameter is known within a certain interval of values and therefore, within this model, the only free parameter of the Morse potential is the stiffness parameter, $\chi$. The well depth $D$ is readily obtained from the condition $V_C(\bar{z}) = V_M(\bar{z})$. For example, if $C_3 = 3.5 \times 10^{-50}\, Jm^3$ and $\chi = 0.5\, \mathring{A}^{-1}$, then $x = 3.13$ and $D = 9.8\, meV$.

The periodic function for the squared pulses is

$$h(x) = \sum_{n=-\infty}^{+\infty} \prod\left(\frac{x - nd}{a}\right) \tag{7}$$

where $a$ is the width of the strips and $d$ the period ($a < d$). The $\Pi(y)$-function is the so-called unit impulse function: 0 for $|y| > 1/2$, 1 for $|y| < 1/2$ and $1/2$ for $|y| = 1/2$. In terms of a

Fourier series, $h(x)$ is expressed as

$$h(x) = \sum_{n=-\infty}^{+\infty} c_n e^{i2\pi nx/d} \tag{8}$$

the corresponding $c_n = c_{-n}$ coefficients being given by

$$c_n \;=\; \begin{cases} \frac{a}{d} & , n = 0 \\ \frac{a}{d} sinc(n\frac{a}{d}) & , n \neq 0 \end{cases} \tag{9}$$

where the normalized *sinc*-function is defined as $sinc(x) = sin(\pi x)/\pi x$. When $d = 2a$, the terms beyond the sixth order are no longer significant. In our case, $d = 20\,\mu m$ and $a = 10\,\mu m$. This Fourier series can also be expressed as

$$h(x) = c_0 \left[ 1 + 2 \sum_{n=1}^{+\infty} sinc(n\frac{a}{d})\, cos(\frac{2\pi nx}{d}) \right]. \tag{10}$$

Finally, the periodic interaction potential thus formed can be expressed as

$$U(x,z) = \sum_{n=-\infty}^{+\infty} V_n(z) e^{i\frac{2\pi nx}{d}} \tag{11}$$

where the first term ($n = 0$) provides the interaction potential $V_0(z) = V(z)$ and the coupling terms ($n \neq 0$) are given by

$$V_n(z) = 2sinc(n\frac{a}{d})V(z). \tag{12}$$

The $c_0$ coefficient can be seen as a scaling parameter and may be ignored.

The CC formalism provides numerically exact quantum reflection probabilities as well as diffraction patterns. The time-independent Schrödinger equation for purely elastic scattering of He atoms with mass $m$ and incident wave vector $\mathbf{k}_i$ is given by

$$\left[ -\frac{\hbar^2}{2m}\nabla^2 + U(\mathbf{r}) - \frac{\hbar^2}{2m}\mathbf{k}_i^2 \right] \Psi(\mathbf{r}) \;=\; 0. \tag{13}$$

Here only in-plane scattering is going to be considered, that is, $\mathbf{r} = (x, z)$. Since the wave function and the interaction potential are periodic, both can be Fourier expanded and one finally reaches a set of coupled equations which reads as

$$\left[\frac{\hbar^2}{2m}\frac{d^2}{dz^2} + \frac{\hbar^2}{2m}k_{n,z}^2 - V_0(z)\right]\Psi_n(z) \;=\; \sum_{n\neq n'} V_{n-n'}(z)\Psi_{n'}(z) \tag{14}$$

with $V_0(z)$ the grating-averaged interaction potential and $\frac{\hbar^2}{2m}k_{n,z}^2$ being the z-component of the kinetic energy of the scattered particles. The squared z-component of the wave vector is written as

$$k_{n,z}^2 \;=\; k_i^2 - \left(k_i \sin\theta_i + \frac{2\pi n}{d}\right)^2. \tag{15}$$

where $\theta_i$ here is, on the contrary, measured wih respect to the normal to the surface. Thus, when comparing with experimental results, theoretical positive $n$ diffraction orders correspond to experimental negative $n$ ones. For every $n$, the effective potential $V_0(z) + \frac{\hbar^2}{2m}(k_i \sin\theta_i + 2\pi n/d)^2$ in Eq.(14) represents a diffraction channel, the second term is the asymptotic energy. This energy depends on $n$ and the incident scattering conditions (energy and polar angle). Open diffraction channels have a positive normal kinetic energy ($k_{n,z}^2 > 0$) while channels which have a negative normal kinetic energy ($k_{n,z}^2 < 0$) are called *closed*. The diffraction probabilities are obtained by solving the CC equations with the corresponding boundary conditions and the intensities are given by

$$I_n = |S_{n0}|^2 \tag{16}$$

where $S_{nn'}$ are the elements of the scattering or collision matrix. These intensities give the probability for an incident wave in the specular channel ($n' = 0$) ending in each one of the open $n$-channels. By construction, the S-matrix is unitary since no Debye-Waller attenuation has been included due to the surface temperature.

The interaction potential given by Equation (4) displays classical turning points due

to the repulsive part of the Morse potential. To distinguish between the phenomenon of quantum reflection and the "normal" reflection from the inner repulsive part of the Morse potential we impose absorbing boundary conditions[10,11] in the inner part. For this purpose, a Woods-Saxon (WS) potential has been introduced in the imaginary part of the diffraction channels

$$V_{WS} = \frac{V_0}{1 + e^{\alpha(z - z_i)}} \tag{17}$$

which is essentially zero in the physical relevant interaction region and turns on sufficiently rapidly but smoothly at the left edge of the grid to absorb the flux over a short distance as possible. We used $V_0 = 0.02\ a.u.$ and $\alpha = 1.2\chi$. As a result, the resulting scattering matrix $\bar{S}$ is no longer unitary. The diffraction intensities are still given by

$$\bar{I}_n = |\bar{S}_{n0}|^2 \tag{18}$$

and the quantum reflection probability is

$$P^{QR} = \sum_n |\bar{S}_{n0}|^2 < 1 \tag{19}$$

for each initial condition. Numerical convergence was obtained by using 61 diffraction channels ($n = -30, \cdots, 30$) with a grid of 10,000 points between -10 $\mathring{A}$ and 210 $\mathring{A}$. Two types of calculations are carried out. First, a one-channel calculation with the specular channel only in order to obtain an estimation of the total reflection probability, and second a multichannel calculation to determine the numerically exact values for the quantum reflected diffraction pattern. Numerical convergence is reached by considering open as well as closed channels, unlike some previous work.[8] Sometimes it is claimed that considering only open channels is justified because quantum reflection occurs far away from the grating where the influence of those channels is expected to be negligible. The presence of closed channels could also be an indication of the importance of the inner region of the potential to describe the quantum

reflection. In any case, this scattering is essentially a multichannel scattering due to the periodicity of the grating.

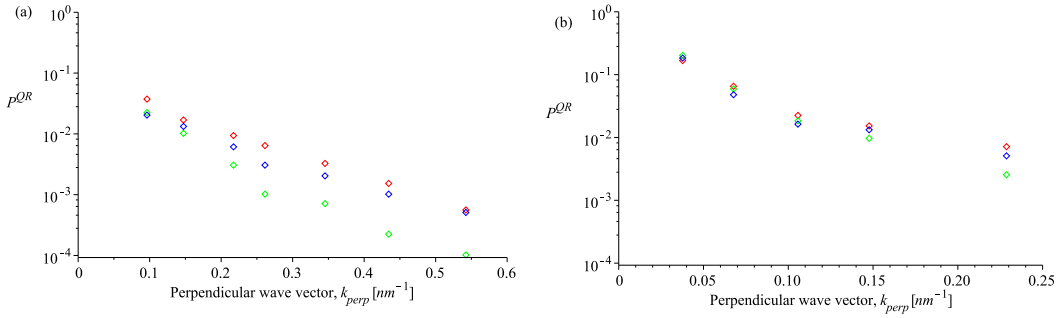


Figure 1: Quantum reflection probabilities are plotted versus the perpendicular incident wave vector (in $nm^{-1}$) for a source temperature of 20 K (a) and 10.8 K (b). Experimental results: red points; one channel (specular) calculation: green points; multichannel calculations: blue points.

In Figure (1), the quantum reflection probabilities are plotted versus the perpendicular incident wave vector for two different source temperatures, 20 K (left panel) and 10.8 K (right panel). Red points represent the experimental values,[3] green points are obtained from a one channel (specular channel) calculation and blue points correspond to the multichannel calculation. The overall agreement is fairly good. These results were reached by fitting the two potential parameters $C_3$ and $\chi$, leading to the values mentioned above. The $C_3$ value is in the expected range for He atoms interacting with a transition metal surface.[3] It should be stressed that, at small perpendicular wave vectors, the one channel (specular) calculation is also quite similar to the same type of calculation reported in[3] where only the attractive Casimir-van der Waals potential is considered in a one-dimensional Schrödinger equation. This equation is solved with a boundary condition that the wave function vanishes at small

$z$ values, that is, small or vanishing distance from the grating. However, as also pointed out in the same reference, at higher perpendicular wave vectors, where He atoms explore deeper regions of the potential well, the agreement with experimental quantum reflection probabilities is rather poor. In these regions, the attractive part is no longer of the type of the Casimir-van der Waals tail. This part is considered in our calculation by means of a Morse potential which should be much more appropriate. In any case, the agreement at any perpendicular wave vector value with the results coming from the multichannel results is fairly good.

These results are only obtained when the absorbing potential is shifted towards the classical turning point of the interaction potential; in particular, at the initial value of the grid $z_i$. Quantum reflection is not observed when the absorbing potential is placed far to the right of the potential well, where the Casimir-van der Waals tail of the interaction potential is prevalent. In other words, the inner part of the interaction potential has a profound effect on the reflection probability, showing that this region cannot be omitted by the $z$-grid integration. To demonstrate this further, we present in Table 1 the multichannel quantum reflection probabilities obtained at an incident energy of 20 $K$ and angle of 3.38 $mrad$ for different values of the Morse well depth D. The badlands region of the long range potential is not affected by these changes.

One may well ask where does this nonlocality appear in the semiclassical analysis of quantum reflection, as presented for example in[7]? We note that the general formulation of quantum reflection always has in it a modification of the semiclassical wavefuncion with an exact solution which is based on nonlocal boundary conditions. When considering scattering from a surface/grating, this condition is that the exact wavefunction vanishes at the surface/grating. When considering potentials which do not have a reflective wall, such as step potentials, the boundary conditions are also nonlocal as they include both transmitted and reflected waves. These nonlocal boundary conditions are essential in deriving the quantum reflection.[12] In other words, the quantum wavefunction necessarily extends into the inner

region of the potential away from the badland region. One cannot claim that it is merely reflected by the badland region. In this context we also note that the reflection coefficient for an Eckart potential well $(-1/cosh(x)^2)$ is zero at *any* energy.[13] In this case, even though the Eckart well has a badlands region typical of an exponential potential, there is no quantum reflection at all. Had the phenomenon of quantum reflection been localized to the badlands region only, then the Eckart potential well would have a finite reflection probability.

**Table 1: The dependence of the multichannel quantum reflection probabilities, $P^{QR}$, on the $D$-parameter of the Morse potential obtained for a source temperature of 20 $K$ and incident angle of 3.38 $mrad$.**

| D (meV) | $P^{QR}$ |
|---|---|
| 7.1 | 1.95 (-2) |
| 8.1 | 1.70 (-2) |
| 10.4 | 1.65 (-2) |
| 11.7 | 1.78 (-2) |
| 14.6 | 2.30 (-2) |

The CC formalism may also be used to compute the diffraction patterns coming from the quantum reflection effect. In principle, there is no reason a priori to expect a one-to-one mapping between good CC quantum probabilities (when comparing to the experimental ones) and the corresponding diffraction patterns. In fact, as shown in Equations (18) and (19), the reflection probability is a global quantity and there are many ways to obtain the same quantity from the sum of diffraction intensities corresponding to the same initial conditions in energy and angle. This is precisely what we observe in our theoretical analysis. In Figure (2), relative diffraction intensities (in %) are displayed as a function of the perpendicular incident wave vector $k_{perp}$ (in $nm^{-1}$) at various source temperatures for $\theta_i = 4.9$ mrad (left plot) and $\theta_i = 7.2$ mrad (right plot). Colored lines are the experimental values obtained from the magnitude of the measured diffraction peak divided by the magnitude of the specular peak. Black numbers label the experimental diffraction orders. Red numbers

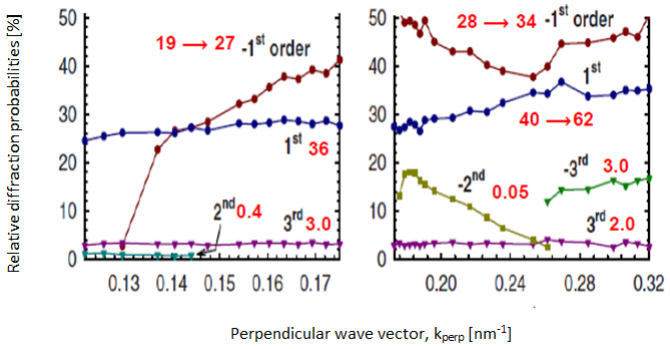


Figure 2: Relative diffraction intensities (in %) as a function of the perpendicular incident wave vector in $\mathrm{nm}^{-1}$, $k_{perp}$ at various source temperatures for $\theta_i = 4.9$ mrad (left plot) and $\theta_i = 7.2$ mrad (right plot). Color lines are the experimental values. Black numbers label the experimental diffraction orders. Red numbers near the diffraction orders correspond to the CC results: a single red number means that in the corresponding interval of $k_{perp}$ the diffraction intensity is nearly constant; $a \to b$ means that in the whole interval of $k_{perp}$, the diffraction intensity displays a smooth variation going from the initial value $a$ to the final value $b$.

near the diffraction orders correspond to the CC results: a single red number means that in the corresponding interval of $k_{perp}$ the diffraction intensity is nearly constant; $a \to b$ means that in the whole interval of $k_{perp}$, the diffraction intensity displays a smooth variation going from the initial value $a$ to the final value $b$. The agreement of the experimental diffraction patterns with the computed ones is not quantitative. However, the qualitative features are present: (i) Important asymmetries in the intensities for positive and negative diffraction orders are noticeable; (ii) Pronounced variations of the diffraction intensities are also found; and (iii) Intensities for the even diffraction orders are quite negligible (for the experimental values up to 18 % but for the theoretical resuts, less than 0.5%). None of these features are found if one neglects the Casimir-van der Waals tail of the interaction potential.

In conclusion, we would like to emphasize the fact that by considering the full grid, in the integration coordinate, as well as appropriate boundary conditions at the edges of the grid, very good quantum reflection probabilities and acceptable diffraction patterns are obtained when comparing to experimental ones, providing also physically acceptable potential parameters. Quantum reflection has been in most cases measured for scattering from surfaces. At

long range, one has a Casimir-van der Waals attractive potential, but at short range, the approaching particle feels the repulsive wall of the surface atoms. This is the justification for the boundary condition that the wave function vanishes for sufficiently small distances from the grating, this boundary condition implies that the quantum reflection is not local to the badlands region alone. Our analysis is consistent if the quantum reflection is considered as a coherent process underlying the nonlocal character of quantum mechanics.

**Acknowledgment**: The authors would like to thank W. Schöllkopf and B. S. Zhao for helpful discussions. This work is supported by a grant with Ref. FIS2014-52172-C2-1-P from the Ministerio de Economia y Competitividad (Spain) and by grants of the Israeli Science Foundation, the Minerva Foundation, Munich and the German Israel Foundation for Basic Research.

## References

(1) Friedrich, H.; Jurisch, A. Quantum reflection times for attractive potential tails. *Phys. Rev. Lett.* **2004**, *92*, 103202.

(2) Pasquini, T. A.; Shin, Y.; Sanner, C.; Saba, M.; Schirotzek, A.; Pritchard, D. E.; Ketterle, W. Quantum reflection from a solid surface at normal incidence. *Phys. Rev. Lett.* **2004**, *93*, 223201.

(3) Zhao, B. S.; Schulz, A.; Meek, S. A.; Meijer, G.; Schöllkopf, W. Quantum reflection of helium atom beams from a microstructure grating. *Phys. Rev. A* **2008**, *78*, 010902(R).

(4) Zhao, B. S.; Meijer, G.; Schöllkopf, W. Quantum reflection of $He_2$ several nanometers above a grating surface. *Science* **2011**, *331*, 892-894.

(5) Kornilov, O.; Toennies, J. P. Matter-wave diffraction of quantum mechanical helium clusters. *Europhysics News* **2007**, *38*, 22-27.

(6) Friedrich, H.; Jacoby, G.; Meister, C. G. Quantum reflection by Casimir-van der Waals potential tails. *Phys. Rev. A* **2002**, *65*, 032902.

(7) Friedrich, H.; Trost, J. Working with WKB waves far from the semiclassical limit. *Phys. Rep.* **2004**, *397*, 359-449.

(8) Stickler, B. A.; Even, U.; Hornberger, K. Quantum reflection and interference of matter waves from periodically doped surfaces. *Phys. Rev. A* **2015**, *91*, 013614.

(9) Sanz, A. S.; Miret-Artés, S. Selective adsorption resonances: Quantum and stochastic approaches. *Phys. Rep.* **2007**, *451*, 37-154.

(10) Seideman, T; Miller, W. H. Calculation of the cumulative reaction probability via a discrete variable representatiion with absorbing boundary consitions. *J. Chem. Phys.* **1992**, *98*, 4412-4422.

(11) Muga, J. G.; Palao, J. P.; Navarro, B.; Egusquiza, I. L. Complex absorbing potentials. *Phys. Rep.* **2004**, *395*, 357-426.

(12) Kohn W. Quantum Mechanics of Sticking, *Surf. Rev. Lett.* **1994**, *1*, 129-132.

(13) Crandall R. E., Exact Propagator for Reflectionless Potentials, *J. Phys. A: Math. Gen.* **1983** *16* 3005-3011.